Carbohydrate doping to enhance electromagnetic properties of MgB2 superconductors

Jung Ho Kim
University of Wollongong, jhk@uow.edu.au

Sihai Zhou
University of Wollongong, sihai@uow.edu.au

Md S. Hossain
University of Wollongong, shahriar@uow.edu.au

Alexey V. Pan
University of Wollongong, pan@uow.edu.au

S X. Dou
University of Wollongong, shi@uow.edu.au

Carbohydrate doping to enhance electromagnetic properties of MgB2 superconductors

Abstract

The effect of carbohydrate doping on lattice parameters, microstructure, T_c, J_c, H_{irr}, and H_{c2} of MgB_2 has been studied. In this work the authors used malic acid as an example of carbohydrates as an additive to MgB_2. The advantages of carbohydrate doping include homogeneous mixing of precursor powders, avoidance of expansive nanoadditives, production of highly reactive C, and significant enhancement in J_c, H_{irr}, and H_{c2} of MgB_2, compared to undoped samples. The J_c for MgB_2+30 wt% $C_4H_6O_5$ sample was increased by a factor of 21 at 5 K and 8 T without degradation of self-field J_c.

Keywords

Carbohydrate, doping, enhance, electromagnetic, properties, MgB2, superconductors

Disciplines

Engineering | Physical Sciences and Mathematics

Carbohydrate doping to enhance electromagnetic properties of MgB$_2$ superconductors

J. H. Kim, S. Zhou, M. S. A. Hossain, A. V. Pan, and S. X. Dou[a]
Institute for Superconducting and Electronic Materials, University of Wollongong, Northfields Ave., Wollongong, New South Wales 2522, Australia

The effect of carbohydrate doping on lattice parameters, microstructure, T_c, J_c, H_{irr}, and H_{c2} of MgB$_2$ has been studied. In this work the authors used malic acid as an example of carbohydrates as an additive to MgB$_2$. The advantages of carbohydrate doping include homogeneous mixing of precursor powders, avoidance of expansive nanoadditives, production of highly reactive C, and significant enhancement in J_c, H_{irr}, and H_{c2} of MgB$_2$, compared to undoped samples. The J_c for MgB$_2$+30 wt % C$_4$H$_6$O$_5$ sample was increased by a factor of 21 at 5 K and 8 T without degradation of self-field J_c. © *2006 American Institute of Physics*. [DOI: 10.1063/1.2358947]

With the relatively high critical temperature (T_c) of 39 K (Ref. 1) and the high critical current density (J_c) of $>10^5$ cm^{-2} in moderate fields, magnesium diboride (MgB$_2$) superconductors could offer the promise of important large-scale applications to be operated at 20 K. A significant enhancement in the electromagnetic properties of MgB$_2$ has been achieved through doping with various forms of carbon (C).[2–6] To take advantage of its T_c of 39 K, enhancements of both the upper critical field (H_{c2}) and J_c are essential. Attempts to accomplish this have invoked the introduction of numerous techniques including chemical doping,[2–6] irradiation,[7] and various thermomechanical processing techniques.[8,9] Chemical doping is a simple and readily scalable technique. Since MgB$_2$ has a relatively large coherence length and small anisotropy, the fluxoids to be pinned are stringlike and amenable to pinning by inclusions and precipitates in the grains.

Among the numerous forms of C-containing dopants, SiC doping has achieved a record high in-field $J_c(B)$, H_{c2}, and irreversibility (H_{irr}) in MgB$_2$.[2] These record high properties have been confirmed and reproduced by many groups,[2,5,10,11] and the performance records remain unbroken up to now. However, the best high-field J_c values achieved in the SiC doped MgB$_2$ wires were compromised by the reduction in self-field and low-field J_c. Although nanosize precursor particles were chosen for the doping process it is a great challenge to achieve homogeneous distribution of a small amount of nanodopants within the matrix materials through solid state mixing. There are always agglomerates of nanoadditives in the precursors. For various forms of C doping, the substitution of C for boron (B) cannot be achieved at the same temperatures as that of the MgB$_2$ formation reaction due to their poor reactivity.

In order to overcome these problems we proposed to use a carbohydrate such as DL-malic acid (C$_4$H$_6$O$_5$) as the dopant. The significant advantages of carbohydrate are as follows. (1) Carbohydrates can be dissolved in a solvent so that the solution can form a slurry with B powder. After evaporating the solvent the carbohydrate forms a coating on the B powder surfaces, giving a highly uniform mixture. (2) The

carbohydrates in the mixture melt at lower temperatures and decompose at temperatures below the formation temperature of MgB$_2$, hence producing highly reactive and fresh C on the atomic scale, as well as a reducing reagent, carbon monoxide, which may convert boron oxide to B, reducing the impurities in B powder. (3) Because of the high reactivity of the freshly formed C, the C substitution for B can take place at the same temperature as the formation temperature of MgB$_2$. The simultaneous dual reactions promote C substitution for B in the lattice and the inclusion of excess C within the grains, resulting in the enhancement of J_c, H_{irr}, and H_{c2}.

In this study, therefore, we used malic acid as a representative of carbohydrate dopant. We fabricated MgB$_2$+C$_4$H$_6$O$_5$ samples with different addition levels. The lattice parameters T_c, J_c, H_{irr}, H_{c2}, and microstructures are presented in comparison with the undoped reference MgB$_2$. MgB$_2$ pellets were prepared by an *in situ* reaction process with the addition of C$_4$H$_6$O$_5$. The selected amount of C$_4$H$_6$O$_5$ (99%), from 0 to 30 wt % of total MgB$_2$ was mixed with an appropriate amount of B (99%) powder in toluene (C$_7$H$_8$, 99.5%). This slurry was dried in vacuum so that the B powder particles were coated by the C coming from C$_4$H$_6$O$_5$. Since the decomposition temperature of C$_4$H$_6$O$_5$ was at around 150 °C, this uniform composite was then mixed with an appropriate amount of Mg (99%) powder. These mixed powders were ground, pressed, and then sintered at 900 °C for 30 min under argon gas. All samples were characterized by x-ray diffraction (XRD), field emission gun-scanning electron microscopy (FEG-SEM), J_c, T_c, H_{irr}, and H_{c2}.[3] The lattice parameters were obtained from Rietveld refinement.

Table I shows the measured data for the undoped MgB$_2$ and MgB$_2$+C$_4$H$_6$O$_5$ samples with different addition levels. The lattice parameters calculated from XRD show a large decrease in the a-axis parameter with 10 wt % C$_4$H$_6$O$_5$ and a small further drop in a with increasing C$_4$H$_6$O$_5$ addition level, but no change in the c-axis parameter. This is an indication of the C substitution for B. The actual C substitution level can be estimated from the a-axis change.[12] It should be noted that the net C percentage addition is only 36% of the C$_4$H$_6$O$_5$ addition. The actual C substitution levels of 1.9–2.3 at % of B at three doping levels are clearly higher than those with other forms of C dopants, which is attributable to the high reactivity of fresh C released from the de-

---

[a]Author to whom correspondence should be addressed; electronic mail: shi_dou@uow.edu.au

TABLE I. Measured data for undoped MgB_2 and $MgB_2+C_4H_6O_5$ samples with different addition levels. H_{irr}^* was calculated from the standard criterion of J_c (100 A cm^{-2}).

| Malic acid ($C_4H_6O_5$) amount (wt %)	Lattice parameters		Actual C (x) in $MgB_{2-x}C_x$[a]	T_c (K)	$\rho_{40\ K}$ ($\mu\Omega$ cm)	$\rho_{300\ K}$ ($\mu\Omega$ cm)	H_{irr}^* (T) (20 K)	J_c (A cm^{-2})	
	a (Å)	c (Å)						Self-field (20 K)	8 T (5 K)
0	3.0835(5)	3.5217(5)		37.6	34.5	73.5	5.4	3.9×10^5	0.1×10^4
10	3.0751(6)	3.5268(3)	0.0380	35.8	90.2	146.5	6.7	3.5×10^5	2.3×10^4
20	3.0746(4)	3.5229(7)	0.0404	35.7	83.8	146.2	6.8	3.5×10^5	2.7×10^4
30	3.0731(9)	3.5214(7)	0.0460	35.8	79.6	131.9	6.7	4.0×10^5	2.6×10^4

[a]Extrapolation from measured lattice parameters (Ref. 12).

composition of $C_4H_6O_5$ at low temperature. The increase in sintering temperature improves both the crystallinity and the C substitution for B. The former will increase T_c, while the latter will decrease T_c. As a compromise, these two opposing factors result in a high level of C substitution for B with a relatively small drop in T_c. The high-field J_c's of the $MgB_2+C_4H_6O_5$ samples were much higher than that of the undoped MgB_2. Specifically, it should be noted that the self-field J_c of $MgB_2+C_4H_6O_5$ samples was not reduced at addition levels as high as 30 wt % $C_4H_6O_5$; hence the connectivity between MgB_2 grains was not affected by addi-

tion with $C_4H_6O_5$. Although there is a possibility of the formation of H_2O during sintering due to the decomposition of $C_4H_6O_5$, there was no degradation in self-field J_c, even for 30 wt % $C_4H_6O_5$ added to MgB_2. This may be attributable to the fact that the decomposition products, C and CO, of $C_4H_6O_5$ reduced B_2O_3 and hence increased the effective cross section of the superconductor.

Figure 1(a) shows the magnetic field dependence of J_c in all samples at 20 and 5 K. It should be noted that J_c values in high field were increased by more than an order of magnitude. For example, the J_c value of 2.5×10^4 A cm^{-2} at 5 K and 8 T for MgB_2+30 wt % $C_4H_6O_5$ sample is higher than that of the undoped MgB_2 by a factor of 21. In addition, there was no J_c degradation in self-field for the MgB_2+30 wt % $C_4H_6O_5$ sample. These findings can be further supported by the flux pinning results. Figure 1(b) plots the field dependence of the volume pinning force, $F_p=J\times B$, of all samples at 20 K. The F_p is normalized by the maximum volume pinning force $F_{p,max}$. The flux pinning for the $MgB_2+C_4H_6O_5$ samples was significantly higher than that of the undoped one at $B>1.5$ T. This result indicates that the $F_p(B)$ of $MgB_2+C_4H_6O_5$ samples was improved by the C substitution effect and nano-C inclusions within the grains.

The normalized temperature dependence of H_{irr} and H_{c2} for all samples is shown in Fig. 2. Significantly enhanced H_{irr} and H_{c2} for $MgB_2+C_4H_6O_5$ samples were observed, suggesting that C substitution into B sites results in an enhancement in H_{irr} and H_{c2}. The steeper slopes of H_{irr} for $MgB_2+C_4H_6O_5$ samples exceeded H_{c2} of undoped MgB_2 below a
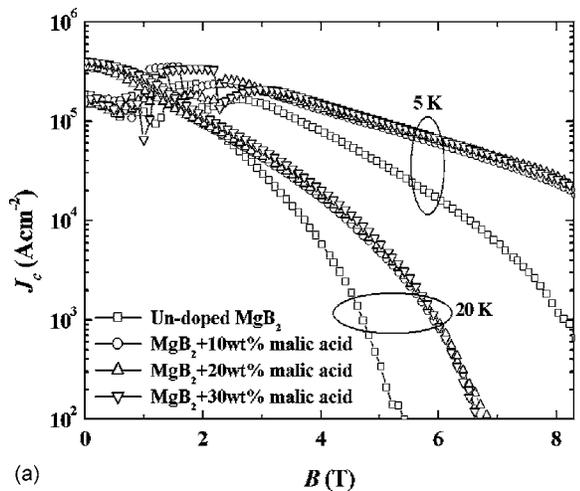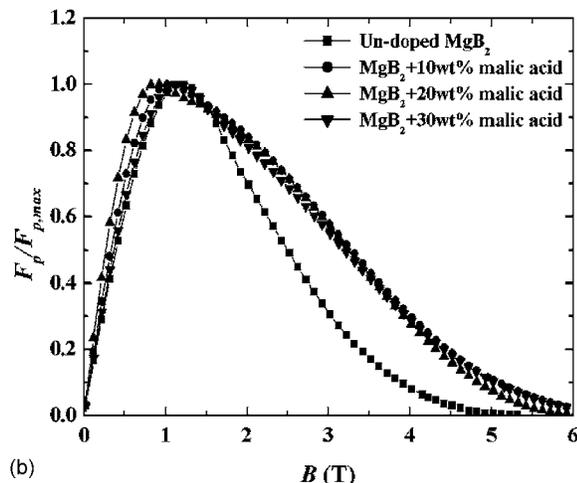
FIG. 1. Superconducting properties of undoped MgB_2 and $MgB_2+C_4H_6O_5$ samples with different addition levels: (a) Magnetic field dependence of J_c in all samples at 20 and 5 K; (b) field dependence of the volume pinning force, $F_p=J\times B$, of all samples at 20 K. The F_p is normalized by the maximum volume pinning force $F_{p,max}$.
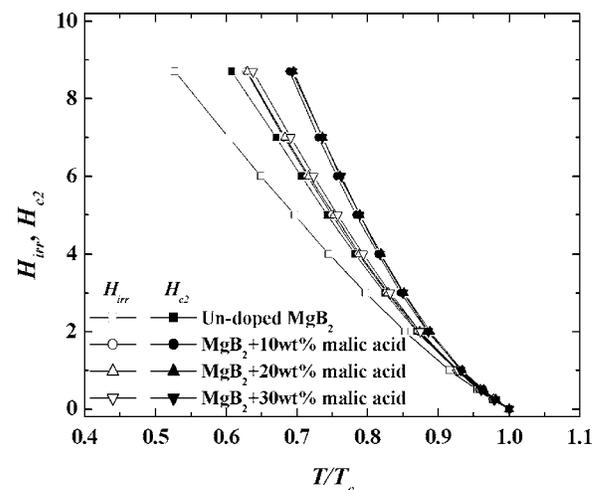

FIG. 2. Normalized temperature dependence of H_{irr} and H_{c2} for undoped and $C_4H_6O_5$ doped samples. H_{c2} and H_{irr} were defined as $H_{c2}=0.9R(T_c)$ and $H_{irr}=0.1R(T_c)$ from the R vs T curve.
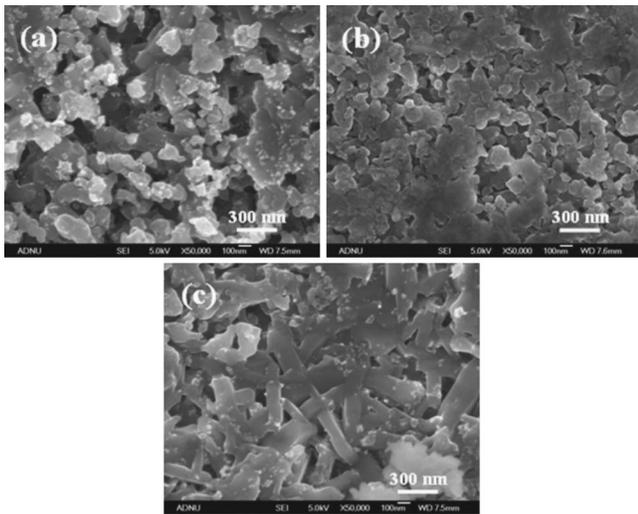
FIG. 3. Photographs from FEG-SEM: (a) Undoped MgB$_2$, (b) MgB$_2$+10 wt % C$_4$H$_6$O$_5$, and (c) MgB$_2$+30 wt % C$_4$H$_6$O$_5$.

FIG. 4. FWHM as a function of the amount of C$_4$H$_6$O$_5$. MgB$_2$(100), (101), (002), and (110) correspond to $2\theta\sim33.6°$, $42.5°$, $52.0°$, and $60.0°$, respectively.

temperature of 22 K. The resistivities ρ for the undoped and MgB$_2$+C$_4$H$_6$O$_5$ samples are 34 and 80–90 $\mu\Omega$ cm at 40 K, respectively, as shown in Table I. The increased resistivity for MgB$_2$+C$_4$H$_6$O$_5$ samples indicates the increased impurity scattering as a result of C substitution into B sites.

FEG-SEM images for (a) undoped MgB$_2$, (b) MgB$_2$+10 wt % C$_4$H$_6$O$_5$, and (c) MgB$_2$+30 wt % C$_4$H$_6$O$_5$ are shown in Fig. 3. The undoped MgB$_2$ sample appears inhomogeneous, consisting of crystalline grains from several tens of nanometers in size to 500 nm. The morphology of the MgB$_2$+10 wt % C$_4$H$_6$O$_5$ sample was refined to smaller, denser, and more homogeneous grains compared to the undoped MgB$_2$ one. The grain refinement by 10 and 20 wt % C$_4$H$_6$O$_5$ additions is supported by the full width at half maximum (FWHM) results for all the peaks, as shown in Fig. 4. As the doping level further increases to 30 wt %, however, grains appear to have a bar/plate shape, with their width up to 150 nm and length up to 400 nm, in a well connected grain network [Fig. 3(c)]. Consistent with the FEG-SEM image is the decrease in FWHM for the 30 wt % doped sample (Fig. 4) although the average FWHM values for all peaks are still bigger than those of the undoped sample. The FEG-SEM image suggests that at higher addition levels C$_4$H$_6$O$_5$ may act as a sintering aid to improve the crystallinity. The grain growth should not improve the electromagnetic properties. However, this effect may be offset by the increase in C substitution level, the reduction in resistivity (Table I), and improvement in grain connectivity. This is well evidenced by the fact that the self-field J_c of the MgB$_2$+30 wt % C$_4$H$_6$O$_5$ sample was enhanced while the improved in-field J_c, H_{irr}, and H_{c2} were maintained, as shown in Figs. 1 and 2.

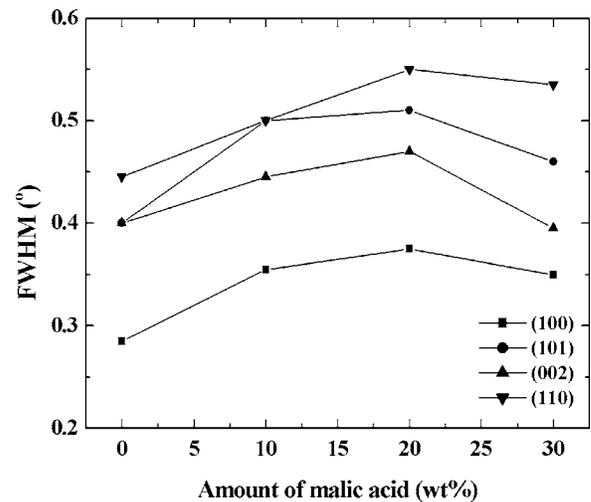In summary, carbohydrate doping results in a small depression in T_c but significantly increases the C substitution level, reduces the impurities, and hence improves J_c, H_{irr}, and H_{c2} performances at all the operating temperatures and over the entire field range. This finding opens a direction for the manufacture of nanodoped materials using the carbohydrate solution route, which solves the agglomeration problem, avoids the use of expensive nanoadditives, and achieves improved performance properties.

[1] J. Nagamatsu, N. Nakagawa, T. Muranaka, Y. Zenitani, and J. Akimitsu, Nature (London) **410**, 63 (2001).
[2] S. X. Dou, S. Soltanian, J. Horvat, X. L. Wang, S. H. Zhou, M. Ionescu, H. K. Liu, P. Munroe, and M. Tomsic, Appl. Phys. Lett. **81**, 3419 (2002).
[3] J. H. Kim, W. K. Yeoh, M. J. Qin, X. Xu, and S. X. Dou, J. Appl. Phys. **100**, 013908 (2006).
[4] R. H. T. Wilke, S. L. Bud'ko, P. C. Canfield, D. K. Finnemore, R. J. Suplinskas, and S. T. Hannahs, Phys. Rev. Lett. **92**, 217003 (2004).
[5] H. Kumakura, H. Kitaguchi, A. Matsumoto, and H. Hatakeyama, Appl. Phys. Lett. **84**, 3669 (2004).
[6] A. Yamamoto, J. I. Shimoyama, S. Ueda, I. Iwayama, S. Horii, and K. Kishio, Supercond. Sci. Technol. **18**, 1323 (2005).
[7] Y. Bugoslavsky, G. K. Perkins, X. Qi, L. F. Cohen, and A. D. Caplin, Nature (London) **410**, 561 (2001).
[8] R. Flükiger, H. L. Suo, N. Musolino, C. Beneduce, P. Toulemonde, and P. Lezza, Physica C **385**, 286 (2003).
[9] A. Serquis, L. Civale, D. L. Hammon, X. Z. Liao, J. Y. Coulter, Y. T. Zhu, M. Jaime, D. E. Peterson, and F. M. Mueller, Appl. Phys. Lett. **82**, 2847 (2002).
[10] H. Yamada, M. Hirakawa, H. Kumakura, and H. Kitaguchi, Supercond. Sci. Technol. **19**, 175 (2006).
[11] M. D. Sumption, M. Bhatia, M. Rindfleisch, M. Tomsic, S. Soltanian, S. X. Dou, and E. W. Collings, Appl. Phys. Lett. **86**, 092507 (2005).
[12] S. Lee, T. Masui, A. Yamamoto, H. Uchitama, and S. Takama, Physica C **397**, 7 (2003).